A&A 554, A79 (2013)
DOI: 10.1051/0004-6361/201321071

Astronomy & Astrophysics

Observational evidence that massive cluster galaxies were forming stars at $z \sim 2.5$ and did not grow in mass at later times

S. Andreon

INAF – Osservatorio Astronomico di Brera, via Brera 28, 20121 Milano, Italy
e-mail: stefano.andreon@brera.inaf.it

Received 9 January 2013 / Accepted 15 March 2013

ABSTRACT

Using *Spitzer* 3.6 micron data we derived the luminosity function and the mass function of galaxies in five $z > 1.4$ clusters selected to have a firm intracluster medium detection. The five clusters differ in richness (ISCS J1438.1+3414 and XMMXCS J2215.9-1738 are twice as rich as ISCS J1432.4+3250, IDCS J1426.5+3508, and JKCS 041) and morphological appareance. At the median redshift $z = 1.5$, from the 150 member galaxies of the five clusters, we derived a characteristic magnitude of 16.92 ± 0.13 in the [3.6] band and a characteristic mass of $\lg M^* = 11.30 \pm 0.05\ M_\odot$. We find that the characteristic luminosity and mass does not evolve between $z = 1$ and $1.4 < z < 1.8$, directly ruling out ongoing mass assembly between these epochs because massive galaxies are already present up to $z = 1.8$. Lower–redshift build–up epochs have already been ruled out by previous works, leaving only $z > 1.8$ as a possible epoch for the mass build up. However, the observed values of m^* at very high redshift are too bright for galaxies without any star formation immediately preceding the observed redshift and therefore imply a star formation episode not earlier than $z_f = 2.5$. For the first time, mass/luminosity functions are able to robustly distinguish tiny differences between formation redshifts and to set *upper* limits to the epoch of the last star-formation episode.

Key words. galaxies: luminosity function, mass function – galaxies: evolution – galaxies: clusters: general – cosmology: observations

1. Introduction

The galaxy mass-assembly history can be reconstructed via the infrared luminosity function (LF), which is sensitive to the growth of the stellar mass of galaxies as a function of time. The available data, almost entirely at $z < 1.2$, are usually interpreted as evidence that that most of the bright galaxies must have also been largely assembled by this redshift (De Propris et al. 1999, 2007; Andreon 2006; Muzzin et al. 2008; Andreon et al. 2009). Andreon (2006) was the first work to sample the high redshift range well (six clusters above $z = 0.99$), and it excluded several mass growth models, in particular a twofold increase in mass over an 8 Gyr period. While consistent with a scenario where galaxies in clusters are fully assembled at high redshift, later works (e.g. De Propris et al. 2007; Muzzin et al. 2008; Strazzullo et al. 2010) are unable to give a more stringent constraint, mainly because a large redshift baseline and precise m^* are needed to distinguish scenarios, whereas very few clusters at high redshift were known, and almost none was present in the studied samples.

At variance with these works, Mancone et al. (2010) studied candidate clusters, i.e. cluster detections, and claim to have finally reached the epoch of galaxy mass assembly. This epoch is at $z \approx 1.3$, because m^* is much fainter at $z \gtrsim 1.3$ than it should be for galaxies if there is no mass growth. We are, according to these authors, seeing the rapid mass assembly of cluster galaxies at $z \approx 1.3$. However, this result is in tension with the K-band LF of the $z = 1.39$ cluster 1WGA J2235.3-2557 (Strazzullo et al. 2010), with the existence of a developed and tight red sequence at even higher redshifts, as high as $z = 1.8$ (Andreon & Huertas-Company 2011; Andreon 2011a,b), and with a very early quenching of the cluster populations (Raichoor & Andreon 2012b). All this evidence implies a peacefully evolution for cluster galaxies up to $z = 1.8$.

Since a number of "bona fide" clusters at high redshift have been discovered in the past very few years and for many of them deep *Spitzer* observations are available, we decided to measure the galaxy mass function of $z > 1.4$ clusters.

Throughout this paper, we assume $\Omega_M = 0.3$, $\Omega_\Lambda = 0.7$, and $H_0 = 70\ \mathrm{km\,s^{-1}\,Mpc^{-1}}$. Magnitudes are quoted in their native system (Vega for I and [3.6] bands, AB for the z' band). Unless otherwise stated, results of the statistical computations are quoted in the form $x \pm y$, where x is the posterior mean and y the posterior standard deviation.

2. The sample and the data

2.1. Sample

In this work we studied the luminosity and mass function of galaxies in $z > 1.4$ clusters with a firm detection of the intracluster medium (ICM). We adopted this choice not to run the risk of including in the cluster sample other high redshift structures that have been named "cluster", but whose nature is uncertain, or just different (e.g. a proto-cluster). Since we are interested in a clean sample of secure clusters, we applied a severe screening to the list of objects generically called cluster in literature, see Sect. 3.3 for discussion, only keeping those with a firm *Chandra* detection of the ICM spatially coincident with a galaxy overdensity. The latter is an unambigous detection of deep potential wells. By our choice, our cluster sample is incomplete. However, our sample would also be incomplete if every structure called cluster were included, because what is available today at very high redshift is a collection of objects, not a complete sample.

Table 1. Cluster sample.

ID	z	t_{exp} [s]
JKCS 041	1.8	1200
IDCS J1426.5+3508	1.75	420
ISCS J1432.4+3250	1.49	1000
XMMXCS J2215.9-1738	1.45	1500
ISCS J1438.1+3414	1.41	1000

The adoption of this criterium leads to five $z > 1.4$ clusters, listed in Table 1, out of the many "cluster" detections in the literature. Our list of $z > 1.4$ clusters does not include the $z \sim 1.5$ cluster by Tozzi et al. (2013) because the available *Spitzer* data sample only part of the cluster and are contaminated by an angularly nearby rich $z = 1$ cluster[1]. Our list does not include the $z = 1.62$ structure claimed by Tanaka et al. (2013) to have an ICM detection because our re-analysis of the deep *Chandra* data available does not confirm their ICM detection after flagging 4 arcsec aperture regions centered on point sources.

The redshift range of bona fide $z > 1.4$ clusters goes from $z = 1.41$ to $z = 1.8$, as detailed in Table 1. All clusters but one have a redshift known with two-digit (at least) precision. Instead, JKCS 041 has a ±0.1 redshift uncertainty, which is the least source of uncertainty in this work because m^* has a negligible change with redshift (i.e. a negligible $\partial m^*/\partial z$) at high redshift. In passing, we note that the presence of a two-digit (spectroscopic) redshift does not necessarily indicate a more precise redshift, as shown by the Gobat et al. (2011) group, whose initial spectroscopic redshift has been lowered by $\delta z = 0.08$ (Gobat 2012[2]), or by MS 1241.5+1710, whose initial spectroscopic redshift has been increased by $\delta z = 0.237$ (Henry 2000).

All the five clusters have *Spitzer* observations. Table 1 lists the object ID (Col. 1), the cluster redshift (Col. 2), and the *Spitzer* exposure time per pixel (Col. 3).

2.2. The data and analysis

The basic data used in our analysis are the standard pipeline pBCD (post Basic Calibrated Data) products delivered by the *Spitzer* Science Center (SSC). These data include flat-field corrections, dark subtraction, linearity, and flux calibrations. Additional steps included pointing refinement, distortion correction, and mosaicking. Cosmic rays were rejected during mosaicking by sigma-clipping. The pBCD products do not merge observations taken in different astronomical observations requests (AORs). AORs are therefore mosaicked together using SWARP (Bertin, unpublished), making use of the weight maps. Images of IDCS J1426.5+3508 were already reduced and distributed by Ashby et al. (2009) so we used them. For the two other clusters at right ascension about 14^h we use the deeper data available in the archive instead.

Sources were detected using SExtractor (Bertin & Arnout 1996), making use of weight maps. Star/galaxy separation was performed by using the stellarity index provided by SExtractor. We conservatively kept a high posterior threshold ($class_{star} = 0.95$), rejecting "sure star" only ($class_{star} > 0.95$) in order not to reject galaxies (by unduly putting them in the star class), leaving some residual stellar contamination in the sample. This contamination is later dealt with statistically, with background and foreground galaxies on the cluster line-of-sight. The use of a high posterior threshold is very different from using a concentration index to select galaxies because the latter at low signal-to-noise or for low-resolution observations is susceptible to (mis)classifing galaxies as stars. Objects brighter than 12.5 mag are often saturated and therefore removed from the sample. No cluster galaxy is that bright.

As pointed out by Ashby et al. (2009), images are already moderately crowed with a 420 s exposure, and this makes the catalog completeness much brighter than the limiting depth (see also Mauduit et al. 2012). Because crowding is greather in cluster regions, incompletness is more severe in these lines-of-sight. For example, a circle of 1 arcmin radius centered on IDCS J1426.5+3508 is 50% overdense compared to the average line-of-sight. The overdensity is higher for richer clusters. Completeness at [3.6] = 19.5 mag is 50% in the general field around IDCS J1426.5+3508 (in agreement with Ashby et al. 2009), but a few percentage points in the cluster (overdense) direction. If neglected, the differential (crowding) correction biases the LF parameters (makes the cluster LF flatter than actually is, and, via the parameter covariance, biases the characteristic magnitude, too). Furthermore, very low values of completeness do not allow reliable LFs to be derived, even when crowding is accounted for by following, for example, Andreon (2001). To avoid the danger associated with an important (cluster-, radial- and magnitude-dependent) crowding correction, we adopted quite bright magnitude limits, corresponding to 90% completeness in average lines-of-sights and we ignored fainter galaxies, as, e.g., in De Propris et al. (2007). The 90% completeness is estimated by comparing galaxy counts in non-cluster lines-of-sight to crowding-corrected galaxy counts taken from Barmby et al. (2008). We checked with the Ashby et al. (2009) data that this procedure returns a completeness vs magnitude estimate that is very close to the one derived by Ashby et al. (2009) from the recovery rate of simulated point sources added in the images. Our threshold magnitudes are very conservative; for example, Mancone et al. (2010, 2012) used 50% completeness magnitude in control field directions, which are about 2 mag fainter than those we would have chosen.

To compute the LF, we adopted a Bayesian approach, as done for other clusters (e.g. Andreon 2002, 2006, 2008, 2010; Andreon et al. 2006, 2008; Meyers et al. 2012). We accounted for the background (galaxies in the cluster line-of-sight), estimated in adjacent lines-of-sight. We adopted a Schechter (1976) LF for cluster galaxies and a third-order power law for the background distribution. The likelihood expression were taken from Andreon et al. (2005), which is an extension of the Sandage et al. (1979) likelihood expression for the case where a background is present. We adopted uniform priors for all parameters, except for the faint end slope α, taken to be equal to -1 for comparison with lower redshift LF determinations. In particular, we took a uniform prior on m^* between 12.5 mag and our adopted (quite bright, indeed) limiting mag. The Bayesian approach allowed us to easily propagate all uncertainties and their covariance into the LF parameters and derived quantities. As a visual check, we also computed the LF by binning galaxies in magnitude bins (e.g. Zwicky 1957; Oemler 1974, and many papers since then). These LFs are plotted in Figs. 1 to 5 as points with errors. Our fit

[1] We note that Tozzi et al. (2013) report having *Spitzer* [3.6] images with exposure time 10 times shorter than the data available in the *Spitzer* archive. Our discovery of the contamination mentioned below uses 970 s long exposure, reduced and analyzed like all the other *Spitzer* data of this work. The contamination has been discovered during the LF analysis.

[2] http://www.sciops.esa.int/SYS/CONF2011/images/cluster2012Presentations/rgobat_2012_esac.pdf

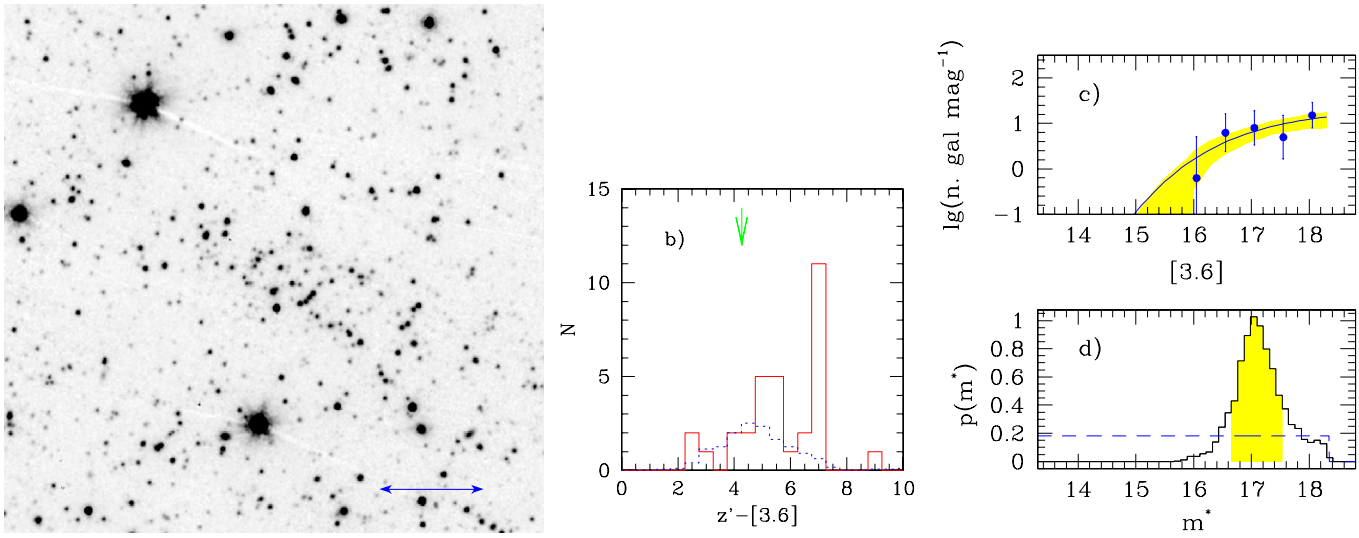

Fig. 1. *Left panel*: [3.6] image of JKCS 041. The field of view is 5×5 arcmin, the ruler is 1 arcmin wide. North is up, east to the left. *Central panel*: color distribution in the cluster line-of-sight (solid red histogram) and in the control field direction (blue dashed histogram). The arrow indicates the expected color of a Grasil young star-forming galaxy (green arrow) at the cluster redshift. *Top-right panel*: luminosity function. The points marks the LF as usually derived in the astronomical literature, whereas the continuous (blue) curve and the shaded area mark the LF and its 68% errors based on our Bayesian analysis. The fit is performed on unbinned data, not on the binned data plotted in this figure. *Bottom-right panel*: probability distribution of m^*. The shortest 68% interval is shaded. The dashed line indicates the assumed prior.

instead used unbinned galaxy counts. For all clusters we adopted an aperture with a 1 arcmin radius (about 500 kpc).

To limit the contamination by galaxies in the cluster foreground, we removed (with one exception discussed in next section) from the sample all galaxies that are too blue to be at the cluster redshift, as in Andreon et al. (2004) and other works (e.g. Mancone et al. 2012). We anticipated that this choice has no impact on the results. For rich clusters, we also computed the LF of galaxies of all colors to check our assumption. To estimate the bluest acceptable color a cluster galaxy may plausibly have, we computed the *optical* − [3.6] color (in the various adopted photometric indexes) of an exponentially increasing star formation history (SFH) model, adopting the SFH of the template named Sc in Grasil. In this way most of the stars at the cluster redshift are newborn. We adopted a formation redshift $z = 3$ (i.e. the template has very young stellar populations, less than 0.8 to 2.3 Gyr old) and a Salpeter initial mass function with lower/upper limit fixed to 0.15/120 $M_\odot$. Grasil (Silva et al. 1998; Panuzzo et al. 2005) is a code to compute the spectral evolution of stellar systems the effects of dust taking into account, which absorbs and scatters optical and UV photons and emits in the IR-submm region.

Optical magnitudes are derived from two sources: for JKCS 041 and XMMXCS J2215.9-1738 we used CFHTLS Deep z' bands (from K-band detected WIRDS catalogs, Bielby et al. 2012). For clusters at right ascension $\sim 14^h$, we used NOAO Deep I band catalogs (Jannuzi & Dey 1999). The data are of adequate depth for our purposes: we have one, or at most two, galaxies detected at [3.6] and undetected in the optical band (because our adoption of a bright magnitude cut in the [3.6] band). For these optically undetected galaxies, their undetection makes their color redder than the blue template and therefore these sources are kept in the sample.

Finally, by integrating the LF we derived the number of cluster galaxies brighter than two limiting magnitudes: a) 18.0 mag, the brighter among all chosen threshold magnitude values. This allows us to properly compare cluster richnesses if m^* does not evolve in the studied redshift range; b) our bright limiting magnitude. This gives the number of cluster galaxies actually fitted. We emphasize that our richnesses computed above accounts for the existence of background galaxies and for errors on, and fluctuation of, the background counts, as well as uncertainties derived from having sampled a finite, usually small, number of cluster galaxies.

3. Results

3.1. Results for individual clusters

3.1.1. JKCS 041 ($z \sim 1.8$)

JKCS 041 (Andreon et al. 2009) stands out quite clearly as remarkable galaxy overdensity in the left-hand panel of Fig. 1. It is the most distant cluster of our sample and also one of the most studied ones thanks to the deep data at various wavelengths. It has been studied in the context of the SZ scaling relations (Culverhouse et al. 2010), and it has been used to measure the evolution of the L_X−T scaling relation (Andreon et al. 2011). JKCS 041 color-magnitude relation has been measured in Andreon & Huertas-Company (2011), whereas the age spread of galaxies on the red sequence is studied in Andreon (2011b). The relation between star formation and environment is determined in Raichoor & Andreon (2012a) and the evolution of the quenching rate with redshift (previously known as Butcher-Oemler effect) in Raichoor & Andreon (2012b).

Because of the presence of a group in the cluster southeastern outskirts (Andreon & Huertas-Company 2011), in our analysis we exclude all the southeastern quadrant of JKCS 041[3]. The red-sequence population also shows up clearly in the z'-[3.6] band (see the central panel of Fig. 1 and compare with the other clusters). The color distribution seems to indicate the presence of a blue population at z'-[3.6] ≈ 5 mag, so redder than the blue spectrophotometric template (vertical arrow), already pointed out using other filters in Raichoor & Andreon (2012a). There is no

[3] A similar contamination is also present for other high redshift clusters, which were not retained in our final sample studied here, such as the $z = 1.393$ 1WGA J2235.3-2557 (Mullis et al. 2005) and the $z \sim 1.5$ CXO J1415.2+3610 (Tozzi et al. 2013) clusters.

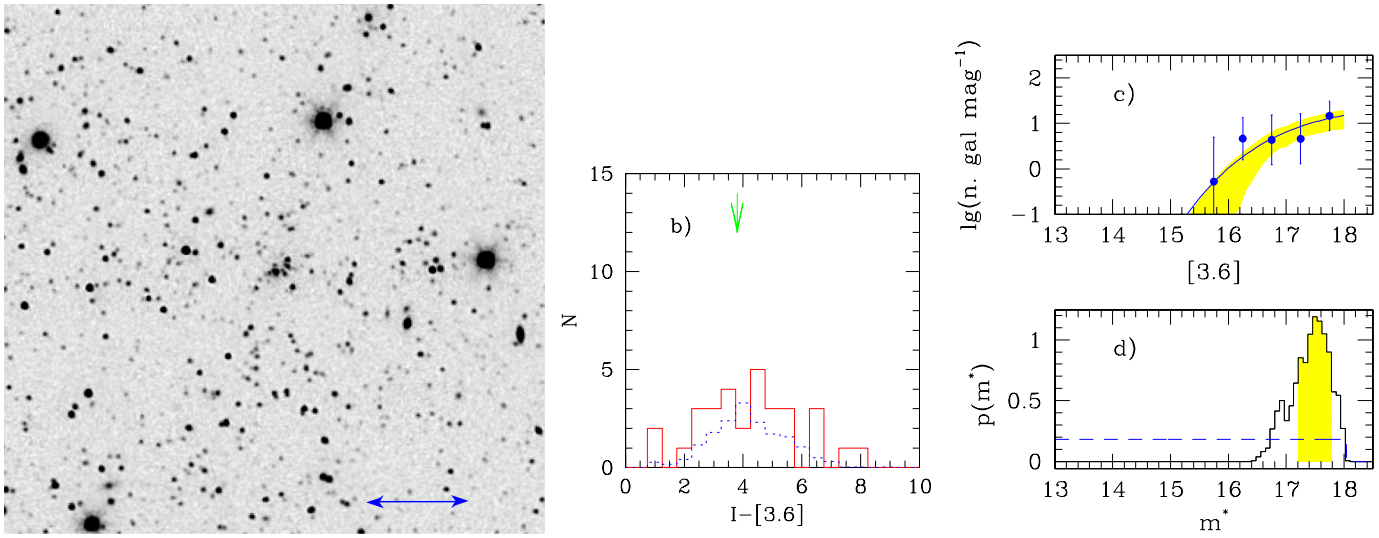

Fig. 2. Same as Fig. 1, but for the cluster IDCS J1426.5+3508.

evidence of an excess of galaxies bluer than the blue template (i.e. left of the vertical arrow in the central panel of Fig. 1).

The LF of those 18 ± 5 galaxies brighter than 18.3 mag in the three quadrants is shown in the top right-hand panel of Fig. 1. The characteristic magnitude is 17.0 ± 0.5 mag (see the bottom right-hand panel for the probability distribution of it). The cluster has a richness of 19 ± 6 galaxies, after accounting for the unused southeastern quadrant.

The LF of red-sequence (i.e. $6.5 < z' - [3.6] < 7.5$ mag) galaxies has an identical characteristic magnitude, 16.9 ± 0.6 mag, as expected because most JKCS 041 galaxies are on the red sequence.

3.1.2. IDCS J1426.5+3508 (z = 1.75)

As also shown in the left-hand panel of Fig. 2, IDCS J1426.5+3508 has a dense core of galaxies, whose clean detection obliged us to remove the image filtering when detecting its galaxies using Sextractor. The cluster has been detected, as JKCS 041 was, as a galaxy overdensity (Stanford et al. 2011). Shallow *Chandra* data (Stanford et al. 2011) allow the ICM to be detected, but not to be characterized (e.g. to estimate its temperature). The ICM is detected in absorption via the Sunyaev-Zeldovich effect by Brodwin et al. (2012). The cluster displays a red sequence (Stanford et al. 2011), not visible in the central panel of Fig. 2, but which shows up, at $I - [3.6] \sim 6$ mag when considering fainter galaxies (our catalog is incomplete at these faint magnitudes, however). Unique among the five clusters considered in this paper, IDCS J1426.5+3508 shows a possible presence of galaxies that are bluer than the blue spectrophotometric template (central panel). For this reason, the LF computation of IDCS J1426.5+3508 uses galaxies of all colors.

The LF of the 15 ± 6 galaxies brighter than 18.0 mag is shown in the top right–hand panel. We find a characteristic magnitude of 17.3 ± 0.4 mag, but we notice that the error amplitude depends on the adopted prior (bottom-right panel): data allow lower values of m^*, although with low probability, but the prior ($m^* < 18.0$ mag) discard them. This situation occurs because the data used are too shallow to bound the lower end of the m^* probability distribution of this cluster. Indeed, IDCS J1426.5+3508 data are the shallowest in our sample (see exposure times in Table 1).

IDCS J1426.5+3508 and JKCS 041 have comparable richnesses (15 ± 6 vs. 19 ± 6 galaxies), although with different color distributions (JKCS 041 has a larger fraction of red galaxies).

3.1.3. ISCS J1432.4+3250 (z = 1.49)

ISCS J1432.4+3250 (left-hand panel of Fig. 3) has, similar to the previous two clusters, been detected as a galaxy overdensity (Brodwin et al. 2011). In terms of spatial distribution, it does not have a compact core of galaxies as IDCS J1426.5+3508 has. Shallow *Chandra* data, presented in Brodwin et al. (2011), allow the detection of the ICM, but not its characterization. The cluster red sequence is studied in Snyder et al. (2012) and also shows up at $I - [3.6] \sim 6$ mag (see the central panel of Fig. 3). Similar to JKCS 041 and unlike IDCS J1426.5+3508, there is no evidence of a galaxy population bluer than the blue spectrophotometric template (see the central panel).

The LF of the 21 ± 6 galaxies brighter than 18.15 mag is shown in the top right–hand panel. We find a characteristic magnitude of 17.4 ± 0.4 mag, but we notice that the error amplitude depends on the adopted prior (bottom-right panel), as for IDCS J1426.5+3508.

ISCS J1432.4+3250 has comparable richnesses (17 ± 5) to the two clusters at higher redshift.

3.1.4. XMMXCS J2215.9-1738 (z = 1.45)

XMMXCS J2215.9-1738 (left panel of Fig. 4) is the most distant X-ray selected cluster (Stanford et al. 2006). The cluster, initially discovered with *XMM-Newton*, has been re-observed with *Chandra* (Hilton et al. 2010), and the original XMM detection was found to be heavily contaminated by point sources (already suspected in XMM discovery data by Stanford et al. 2006). Although X-ray selected, hence likely overbright for its mass and temperature (Andreon et al. 2011), the cluster turns out to be underluminous for its temperature assuming a self-similar evolution (Hilton et al. 2010: Andreon et al. 2011). Its color-magnitude relation is studied in Hilton et al. (2009) and Meyers et al. (2012).

The cluster's red sequence shows up at $z' - [3.6] \sim 6.5$ mag (see the central panel of Fig. 4). Unlike IDCS J1426.5+3508, there is no evidence of a galaxy population bluer than the blue

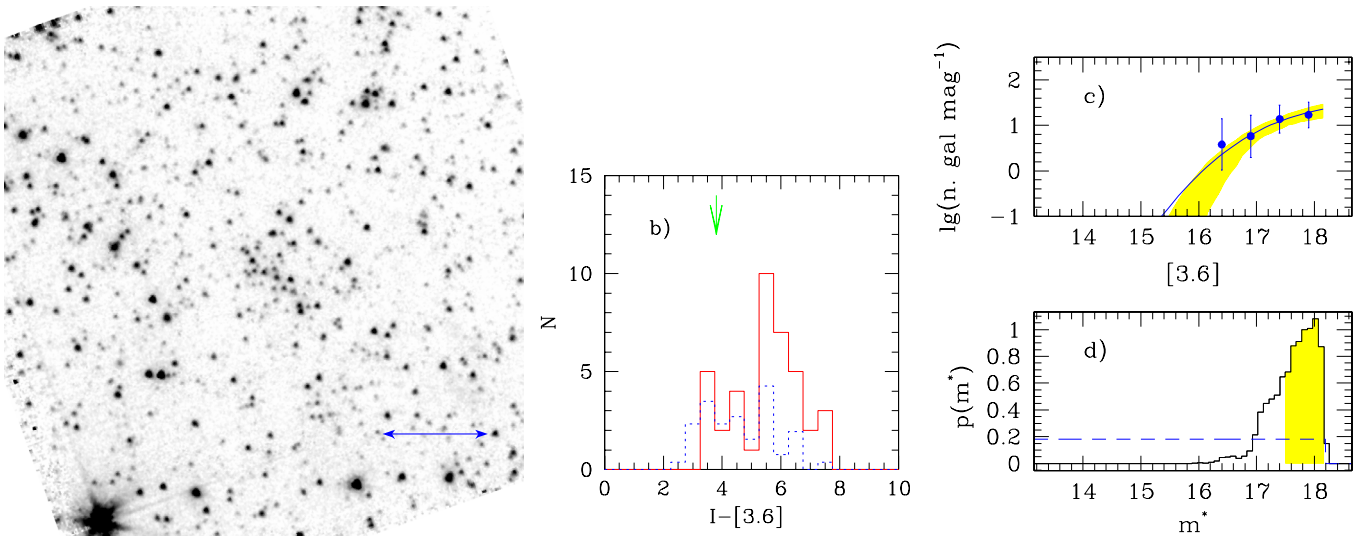

Fig. 3. Same as Fig. 1, but for the cluster ISCS J1432.4+3250.

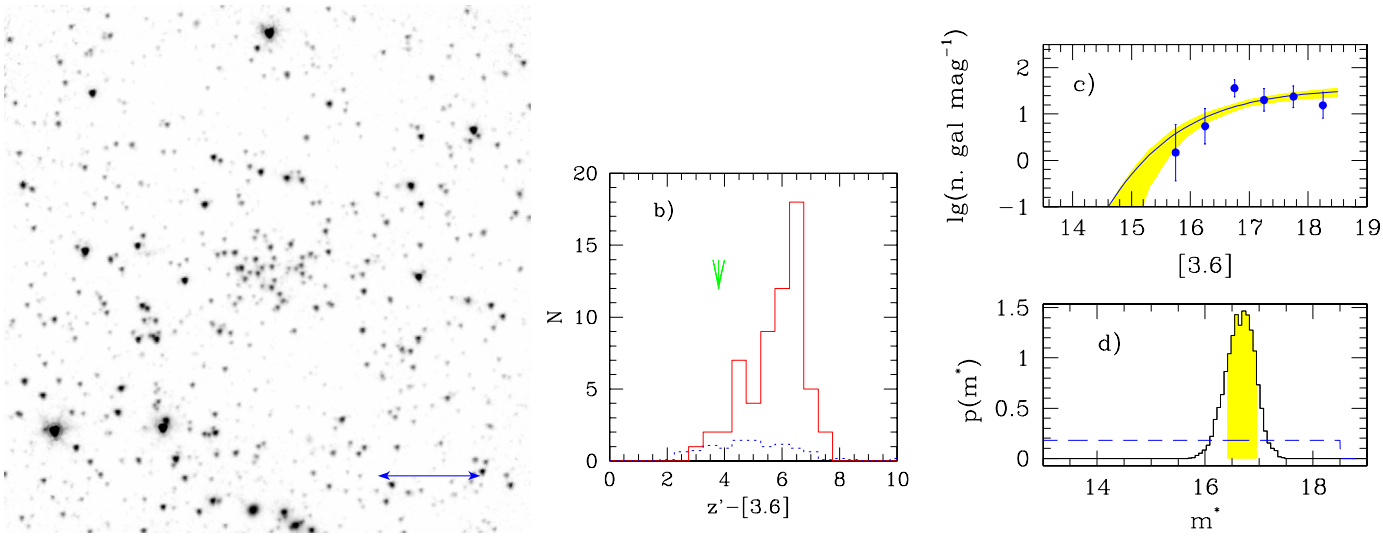

Fig. 4. Same as Fig. 1, but for the cluster XMMXCS J2215.9-1738.

spectrophotometric template (see the central panel). The LF of the 49 ± 8 galaxies brighter than 18.5 mag is shown in the top right-hand panel. We find a characteristic magnitude of 16.6 ± 0.3 mag (see the bottom right-hand panel for the probability distribution of it). ISCS J1432.4+3250 is richer than the other clusters at higher redshift (36 ± 6 vs. 15 to 20 galaxies).

Richnesses and characteristic magnitude of the LF derived removing the color selection are indistinguishable from those just derived (see Table 2) because of the large dominance of red galaxies.

This cluster, at the spectroscopic redshift $z = 1.45$, has a red sequence 0.5 mag bluer than JKCS 041, independently confirming that JKCS 041 has $z > 1.45$ and that therefore JKCS 041 has to be kept in the sample of $z > 1.4$ clusters[4]. We emphasize that this color comparison uses homogeneous photometry that is uniformly reduced (z' band by Bielby et al. 2010, this work for [3.6] band).

[4] After the paper acceptance, JKCS 041 has been spectroscopic confirmed to be at high redshift by mean of HST spectroscopy.

3.1.5. ISCS J1438.1+3414 ($z = 1.41$)

ISCS J1438.1+3414 (left-hand panel of Fig. 5) has been detected as a galaxy overdensity (Stanford et al. 2005). Deep *Chandra* data (Andreon et al. 2011) allowed characterizing the ICM and measuring the evolution of the L_X−T scaling relation (Andreon et al. 2011). Its red sequence has been studied in Meyers et al. (2012). The cluster red sequence stands out (see the central panel of Fig. 5), although it seems quite broad. However, to accurately measure the width of the red sequence, a more tailored measurement of color is needed. Unlike IDCS J1426.5+3508, there is no evidence of a galaxy population bluer than the blue template (see the central panel).

The LF of the 47 ± 8 galaxies brighter than 18.15 mag is shown in the top right-hand panel. We find a characteristic magnitude of 16.8 ± 0.3 mag. The cluster is quite rich, 42 ± 7 galaxies brighter than 18 mag, as rich as XMMXCS J2215.9-1738, and much richer than the clusters at higher redshift. Richnesses and characteristic magnitude of the LF derived by removing the color selection are indistinguishable from those derived above (see Table 2) because of the strong dominance of red galaxies.

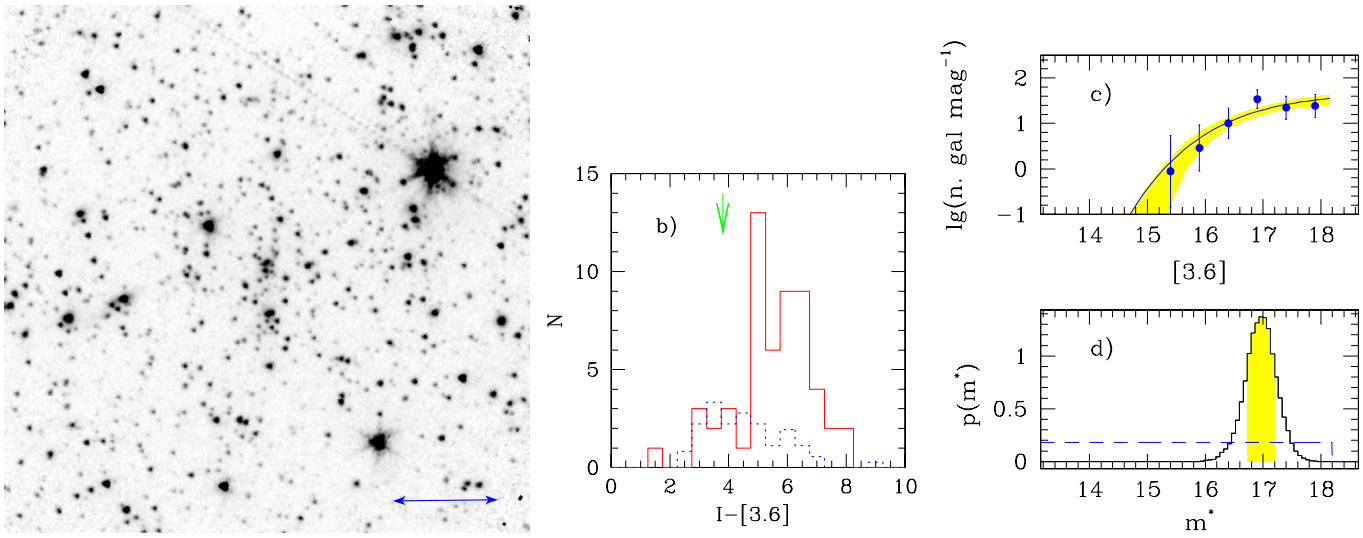

Fig. 5. Same as Fig. 1, but for the cluster ISCS J1438.1+3414.

Table 2. Results.

ID (1)	m^* (2)	n(<18.0) (3)	Ref mag (4)	n(<ref mag) (5)	Notes
JKCS 041	17.0 ± 0.5	19 ± 6	18.30	18 ± 5	$z' - [3.6] > 4.3$ mag
IDCS J1426.5+3508	17.3 ± 0.4	15 ± 6	18.00	15 ± 6	galaxies of all colors
ISCS J1432.4+3250	17.4 ± 0.4	17 ± 5	18.15	21 ± 6	$I - [3.6] > 3.8$ mag
XMMXCS J2215.9-1738	16.6 ± 0.3	37 ± 6	18.50	52 ± 8	$z' - [3.6] > 3.8$ mag
ISCS J1438.1+3414	16.8 ± 0.3	42 ± 7	18.15	47 ± 8	$I - [3.6] > 3.8$ mag
Other fits					
JKCS 041	16.9 ± 0.6	13 ± 4	18.30	12 ± 4	$6.5 < z' - [3.6] < 7.5$ mag
XMMXCS J2215.9-1738	16.5 ± 0.3	38 ± 6	18.50	52 ± 8	galaxies of all colors
ISCS J1438.1+3414	16.8 ± 0.3	43 ± 8	18.15	47 ± 9	galaxies of all colors

Notes. Richnesses in Col. (5) of JKCS 041 refers to measurement in three quarters of the cluster area, see text.

3.2. Collective analysis

Figure 6 shows the derived m^* values of the five $z > 1.4$ clusters, as well as previous determinations from the literature in the [3.6] band (Andreon 2006; Muzzin et al. 2008; Mancone et al. 2010, 2012; Stalder et al. 2013), corrected in the case of Muzzin et al. (2008) for the different faint end slope adopted. Andreon (2006), Muzzin et al. (2008), and Mancone et al. (2010) fitted, as we also do, an LF with a fixed slope. The plotted errors are heterogeneous and not easily comparable because they do not include the same terms in the error budget. In particular, the Mancone et al. (2010) results are based on a few spectroscopically confirmed clusters and many putative cluster detections, including false ones, as mentioned by the authors. At $z < 1.2$, Muzzin et al. (2008) is consistent with the more precise determination of Andreon (2006), whereas Mancone et al. (2010) m^* values display a slower change with redshift than the other data. The difference is statistically significant if one assumes that the Mancone et al. (2010) errors are correctly estimated.

The five $z > 1.4$ clusters studied in this paper (black open dots) have m^* values that are consistent among themselves. We therefore combined the data of the five clusters by multiplying their likelihoods after tying the characteristic magnitude parameters. We find $m^* = 16.92 \pm 0.13$ at $z = 1.5$, the median redshift of the six clusters (solid dot), based on the 150 member galaxies of the combined sample. This value is is 0.8 mag brighter than the values measured by Mancone et al. (2010) in the same redshift range. The difference is statistically significance if one assumes that the Mancone et al. (2010) errors are correctly estimated. As detailed in the technical appendix, we identify the likely reason for the disagreement, Mancone et al. (2010) did not adopted the

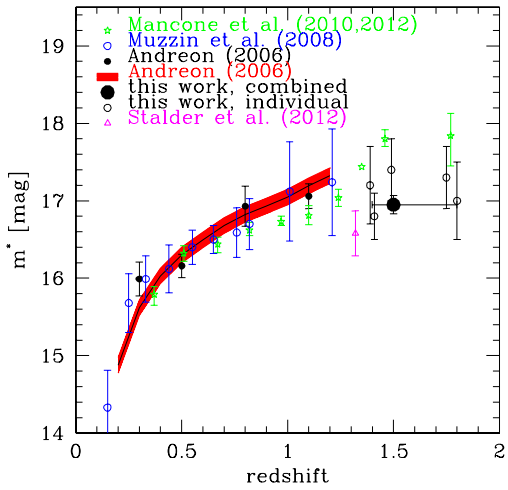

Fig. 6. Characteristic magnitude vs. redshift: observed values from Andreon (2006, two derivations shown as solid small points and as shading), Muzzin et al. (2008, open blue points, $z < 1.3$), Stalder et al. (2013), and Mancone et al. (2010, 2012). Error bar are not easy to compare across works because they do not include the same terms in the error budget.

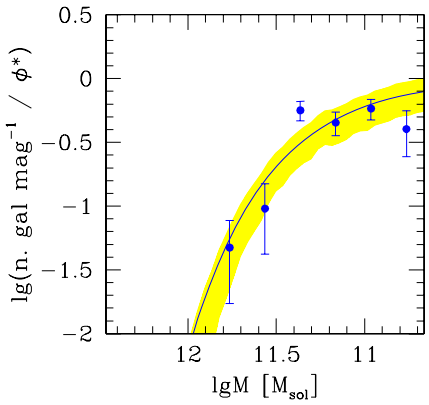

Fig. 7. Combined mass function of the six $z > 1.4$ clusters. Data points and error bars are computed as usual (e.g. Oemler 1973, see Sect. 2.2). The solid line is the mean model, the shaded region indicates the 68% uncertainty of the model.

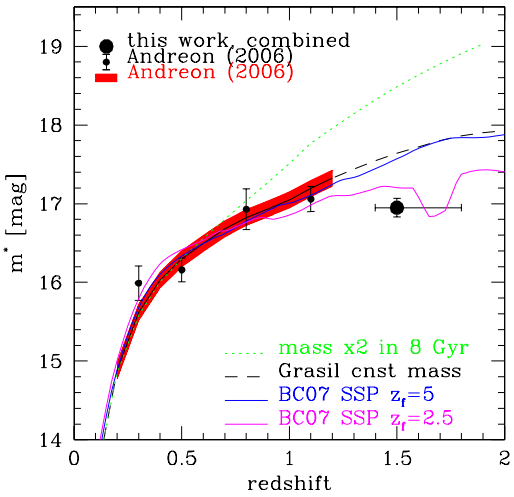

Fig. 8. Characteristic magnitude vs. redshift, with several model predictions.

likelihood expression appropriate for the data used, and we also exclude the possibility that the difference is due to an intrinsic variance of M^*.

We emphasize that in this combined fit, the precise redshift of the five clusters is irrelevant, provided they have $z > 1.4$. Therefore, the lack of a spectroscopic redshift for JKCS 041 (or any other cluster) is not detrimental for the collective m^* determination (or for individual m^*, as it is self-evident). We also emphasize that the highest redshift cluster, JKCS 041, only contributes 10% of the total number of galaxies, and that an indistinguishable result would therefore be found by dropping it from the sample.

Figure 7 plots the galaxy mass function of the combined five clusters. Mass is defined as the integral of the star formation rate, and it is derived from the [3.6] luminosity assuming a single stellar population (SSP) formed at $z_f = 2.5$, modeled by the 2007 version of Bruzual & Charlot (2003) spectrophotometric population synthesis code with solar metallicity and a Chabrier (2003) initial mass function. Based on the 150 member galaxies of the combined sample, the mass function is determined with a 40% error in the $10.5 < \lg M < 12\ M_\odot$ range. The characteristic mass is $\lg M^* = 11.30 \pm 0.05\ M_\odot$, where the error does not account for the systematic errors coming from the conversion from luminosity to mass (e.g. about the stellar initial mass function shape).

Figure 8 summarizes the observational data by keeping m^* determinations limited to confirmed clusters (Muzzin et al. 2008 and Mancone et al. 2010 studied a mix of real clusters and cluster detections) and setting the Mancone et al. (2012) and Stalder et al. (2013) determinations aside because these works use galaxy counts in a magnitude regime where a crowding correction is, at best, compelling, but ignored (see also the technical appendix). The characteristic luminosity m^* has the same value at $1.4 < z < 1.8$ as at $z \sim 1$. This is the main result of this work, which still holds true when keeping all $z < 1.3$ data (see Fig. 6).

Figure 8 also plots the luminosity evolution expected for several mass-growth histories. The very steep luminosity evolution drawn in the figure (dotted curve) is a Grasil model in which the mass doubled in the last 8 Gyr, first explained and then ruled out in Andreon (2006). Mass-evolving models are rejected by the data, because a mass growth makes galaxies brighter (because more massive) at lower redshift, and thus these models do not fit the data. For example, exponentially declining τ models are rejected by the data for all τ tau values higher than 0.5 Gyr, the precise value depending however on the adopted z_f. Models involving mergers do not fit the data because the latter makes descending galaxies more massive and therefore brighter, i.e. moves m^* to brighter values going to lower redshift, while the points at "low" ($z \sim 1$) redshift are too faint for the $1.4 < z < 1.8$ point(s).

Therefore, from now on we only consider models with no ongoing (in the last 11 Gyr) mass growth. The solid line shows the luminosity evolution of an SSP, modeled as previous SSP but formed at $z_f = 5$. The dashed line close to this SSP is a Grasil non-evolving mass model (named E both in the Grasil package and in Andreon 2006). This model is a bit more physical than Bruzual & Charlot (2003) because, for example, a metallicity evolution is allowed during the 1 Gyr long star formation episode started at $z = 5$ (all other Grasil parameters are kept to the default value). These models are rejected too by the data, being too faint at very high redshift (or too bright at lower redshift if models are normalized at $1.4 < z < 1.8$). To have an overall flat evolution at $z \gg 1$ and the observed trend at $z \lesssim 1$, one needs to boost the light at $1.4 < z < 1.8$ without increasing the cluster mass, otherwise the descending galaxies would be too massive (bright) for the low ($z \lesssim 1$) redshift data points. This can be achieved by considering an SSP with a formation redshift very close to the highest observed redshift, $z_f = 2.5$, a mere 0.9 Gyr age difference from the age of the two most distant clusters in the sample. To boost the light observed at $1.4 < z < 1.8$, and thus emitted at early ages (1 to 2 Gyr), it is necessary to use the 2007 version of the Bruzual & Charlot (2003) models or Maraston (2005) and to keep a low z_f. In fact, the 2003 release of Bruzual & Charlot (2003) gives galaxies that are too faint (for the data) galaxies in the critical 1 to 2 Gyr age because of the different treatment of the thermally-pulsing asymptotic giant branch (TP-AGB). Larger z_f does not boost the light enough to reproduce the data: the $z_f = 5$ case is dipicted in the figure and does not fit the data. Similarly, a $z_f = 3$ SSP does not fit the data.

To summarize, models with mergers or recent star formation (in the past 11 Gyr) are rejected because they are too luminous at mid-to-high z (or, equivalently, too faint at very hight redshift). Populations that are too old (SSPs with $z_f = 5$) are rejected because too faint at very high z. The similarity of m^* at $1.4 < z < 1.8$ and $z \sim 1$ implies an assembly time earlier than $z = 1.8$ and, at the same time, a star formation episode that is not much earlier than $z_f = 2.5$ in order to boost the luminosity of the galaxies observed between 0.9 to 2.0 Gyr after it (our $1.4 < z < 1.8$ galaxies).

Past works dealing with luminosity/mass functions usually give a *lower* limit on the formation redshift or on the last star-formation episode. The large redshift baseline and the robustly measured m^* values of this work are able to distinguish SSPs with $z_f = 2.5$ or $z_f = 5$ (in Fig. 8 these SSPs are hardly distinguishable below $z \sim 1.2$ and widely different at higher redshift), and are also able to indicate that the *upper* limit of the latest star formation episode did not preceed the redshift of the two most distant clusters in the sample by a long time, only about 0.9 Gyr.

We emphasize that exponentially declining models with small τ (e.g. 0.1 Gyr) show a luminosity evolution very similar to SSP models, and thus are an equally acceptable fit to the data. Similarly, models with twice the solar metallicity are hardly distinguishable in Fig. 8 from solar metallicity models, so are also acceptable. However, adopting them does not change our conclusion. Finally, we note that the impact of TP-AGB stars on galaxy spectral energy distributions is still under discussion (Zibetti et al. 2011): the lower their contribution to the overall emission in the rest-frame near-infrared band is, the harder it is to fit our data.

3.3. Cluster choice

To be included in this work, a $z > 1.4$ structure should have a firm, *Chandra*, ICM detection that is spatially coincident with a galaxy overdensity. This may seem overly restrictive, and in fact at an early stage of this work we considered other possible criteria, but we found them unsuitable.

Initially, we accepted $z > 1.4$ spectroscopic confirmed clusters. However, relying on the common "spectroscopic confirmation" to name a cluster is dangerous at high redshift: the presence of a spectroscopically confirmed cluster-sized galaxy overdensity is not a guarantee of the presence of a cluster. It is enough to think about the zoo of structures with different names (proto-clusters, redshift spikes), often with several concordant redshifts in areas of a few Mpc^2. The usual spectroscopic criteria have been shown to have low reliability by Gal et al. (2008) using a real spectroscopic survey. This is exemplified by the spectroscopic confirmation of the Gobat et al. (2011) $z = 2.07$ group: recent spectroscopic data (Gobat et al. 2012[5]) show that none of their original 11 spectroscopic members used to spectroscopically confirm the group belong to the group, all being more than 8000 km s^{-1} away from the group. Given the danger of the "spectroscopic confirmation", we choose to require a firm ICM detection.

Later, we considered a suitable definition of cluster to be every galaxy overdensity with a spatially coincindent X-ray detection, either from *Chandra* or XMM. However, a weak XMM detection, typical of most clusters in the XMM Deep Cluster Survey (Fassbender 2011) and of other searches, such as Henry et al. (2010), is an ambigous cluster detection: it may be ICM emission or an AGN misclassified as extended source because of the low XMM resolution and the low signal-to-noise. This is the case of the Papovich et al. (2010) structure, initially named cluster, and renamed proto-cluster in Papovich et al. (2012). It was detected as a 4σ XMM source (as many Fassbender 2011 "clusters"). Later pointed *Chandra* follow-up observations revealed a bright point source and no extended emission (Pierre et al. 2012) using observations planned to measure the ICM temperature to better than 30% out to r_{500} (M. Pierre *Chandra* proposal abstract). Similarly, the Gobat et al. (2011) group with a 3.5σ XMM detection after point source subtraction is undetected in deep *Chandra* observations (Gobat et al. 2011).

Therefore, to avoid the risk of computing the LF of an environment mis-identified as a cluster, i.e. of comparing "apples" (at high redshift) to "oranges" at low redshift (Andreon & Ettori 1999), we asked for a firm, *Chandra*, ICM detection that is spatially coincident with a galaxy overdensity. The superb *Chandra* angular resolution allows X-ray point sources (1″ wide) to be easily recognized from extended (20″ wide) ICM emission, even in the low signal-to-noise regime, unlike XMM.

4. Summary

We analyzed deep *Spitzer* data of the five $z > 1.4$ clusters with a firm detection of the ICM spatially coincident with a galaxy overdensity. This definition of cluster gets rid of the many sorts of cluster-sized structures known at high redshift (such as proto-cluster), which may differ from clusters and allows us to be certain we are comparing "apples to apples" (Andreon & Ettori 1999). The analyzed data are deep (about 1000 s), but to avoid a cluster- radial-magnitude-dependent, unreliable crowding correction, we only consider bright galaxies (brighter than 18.0−18.5 mag), about 2 mag brighter than other authors would choose for data with the same exposure time. The five clusters differ in richness (ISCS J1438.1+3414 and XMMXCS J2215.9-1738 are twice richer than ISCS J1432.4+3250, IDCS J1426.5+3508 and JKCS 041) and morphological appareance. By adopting the correct expression of the likelihood for the data in hand we derived the LF in the [3.6] band and the characteristic magnitude m^*, the latter by marginalizing over the remaining parameters except α. Since the five m^* values are found to be consistent with each other, we combined the data in the unique statistically acceptable way, by multiplying the likelihood of each individual determination. We found a characteristic luminosity of $m^* = 16.92 \pm 0.13$ at $z = 1.5$, the median redshift of the six clusters. Assuming a luminosity-to-mass conversion fixed by an SSP with $z_f = 2.5$, we found a characteristic mass $\lg M^* = 11.30 \pm 0.05$ at $z = 1.5$ and a mass function determined with about 40% error in the $10.5 < \lg M < 12\ M_\odot$ range from the 150 member galaxies of the combined sample.

We found that the characteristic luminosity and mass does not evolve between $z \sim 1$ and $1.4 < z < 1.8$, directly ruling out ongoing mass assembly between these epochs because massive galaxies are already present at $z = 1.8$. Lower redshift build-up epochs were already ruled out by previous works, leaving only $z > 1.8$ as a possible epoch for the mass build-up. Populations that are too old (SSPs with $z_f = 5$) are rejected because they are too faint at very high z. The observed values of m^* at very high redshift are, however, too bright for galaxies without any star formation shortly preceding the observed redshift. The similarity of m^* at $1.4 < z < 1.8$ and $z \sim 1$ implies a star formation episode no earlier than $z_f = 2.5$ in order to boost the luminosity of the galaxies observed at $1.4 < z < 1.8$ without increasing their mass. For the first time, mass/luminosity functions are able to robustly distinguish tiny differences between formation redshifts ($z_f = 2.5$ from $z_f = 3$) and to set *upper* limits to the last star formation episode. This did not preceed the redshift of the two most distant clusters in the sample by a long time, only about 0.9 Gyr. In short, $1.4 < z < 1.8$ is the post star-forming age of massive cluster galaxies, we found that massive cluster galaxies were still forming stars at $z \sim 2.5$ and that they did not grow in mass at later times.

[5] http://www.sciops.esa.int/SYS/CONF2011/images/cluster2012Presentations/rgobat_2012_esac.pdf

Acknowledgements. This work is based on observations made with the *Spitzer* Space Telescope.

Appendix A: Technical addedum about the LF determination

Methods for deriving the luminosity function date back to Zwicky (1957) at least, with newer methods usually more properly addressing the complicate features of the astronomical data not considered by previous methods (see Johnston 2011 for a detailed list of references and Andreon 2011a for a listing of many of the awkward features of the astronomical data). For challenging estimations such as those of high redshift clusters, these "complications" include the use of the correct likelihood expression for the handled data and, in the case of deep data, the (radial- magnitude- cluster-dependent) crowding corrections or the adoption of a bright limiting magnitude. If the objects used to build the LF include putative clusters (i.e. spurious or false cluster detections) or objects of a different nature from clusters (e.g. filaments), this uncertainty should be folded into the likelihood expression. The same is true if clusters have a photometric redshift, unless m^* is constant in the redshift uncertainty range. If galaxies are selected with photometric redshift or their photometric redshift is used in the LF determination, uncertainties (both statistics and systematics) should be folded into the likelihood expression, too. Both effects introduce a bias on m^* if neglected, and this can be easily appreciated by remembering that contamination and photometric redshift errors work as a convolution filter making the LF broader, thus biasing m^* even in the simplest case (symmetric errors). Complicated bias patterns are introduced when asymmetry is important. If galaxies without optical counterparts are excluded from the LF computation, the likelihood expression should be modified to correct for the bias induced by the forced optical detection requirement.

Mancone et al. (2010, 2012) faced most of these issues but did not adopt the likelihood appropriate for the data used. This is the reason, in our opinion, for the (formally statistically) different m^* change with redshift at $z < 1.2$ between Mancone et al. (2010) and the other works, as well as for the (formally statistically) different m^* values between Mancone et al. (2010) and this work at $z \sim 1.5$. Before interpreting them as genuine differences, due for example to two populations of clusters with widely different m^* values, with Mancone et al. (2010) primarly sampling one population and this work the other, one should first make certain that all determinations are robustly derived and refer to clusters as we usually intend them (the author consider sheets, filaments, proto-clusters, and false cluster detections as fairly different from clusters), and second, three of the five clusters studied in this work are likely also in the Mancone et al. (2010) sample (using shallower data, however).

For completeness, we also explored whether the difference between our m^* values and those in Mancone et al. (2010) at $z \sim 1.5$ may be due to an intrinsic variance of M^* values. By performing a Monte Carlo simulation, we computed the probability that if M^* has an intrinsic scatter, five out five of the clusters studied in this work are all within 0.6 mag, and the m^* of the combined cluster is 0.85 mag brighter (or more) than the Mancone et al. (2010) value. To this aim, as prior probability distribution for the intrinsic (i.e. accounting for measurement errors) scatter at $z \sim 1.5$ we adopted the posterior probability distribution computed for the 17 clusters at $0.29 < z < 1.06$ in Andreon et al. (2004), whose LFs have been fitted by holding α fixed, as we and Mancone et al. (2010) both do. This distribution may be approximated by a normal distribution centered on 0.02 mag, with sigma 0.22 mag and truncated at zero. The distribution is quite broad, meaning that we allow the possibility in our simulations that the instrinsic scatter may be very large. In fact, 5% of our simulations have an intrinsic M^* scatter larger than 0.4 mag. Note that in simulations we adopted the actual probability distribution, not the Normal approximation mentioned above. Then, we generated 60 000 simulated data sets, each one composed of five clusters, with m^* values having the same errors as our observed values and having Mancone et al. (2010) mean m^* (and intrinsic scatter as detailed above). Finally, we counted how many times we observe mean m^* offsets in the simulated data larger than those in the real data (0.85 mag) and individual m^* values all within 0.6 mag (the observed maximal difference between the individual m^* measured by us). We found no case in 60 000 simulations, i.e. the probability of observing a larger disagreement because of the intrinsic variance in M^* is a negligible 2×10^{-5}.

To allow a possible evolution of the intrinsic scatter between the redshift where it is measured, $0.3 < z < 1.1$, and the redshift where we need to known its value, $z \sim 1.5$, we performed other simulations assuming that at higher redshift the intrinsic scatter is twice higher (if we reduce the scatter at higher redshift, it becomes even more implausible to observe the observed m^* offset). Also in this case, we found no case matching the observations out of our 60 000 simulations. In short, it is very unlikely that the intrinsic scatter on M^* is the source of the disagreement between $z \sim 1.5$ determinations in these two works.

We emphasize that our search for a physical reason that explains differences in the mean m^* assumes that measurements and errors (i.e. the likelihood) are (is) correct whereas those in one of the compared works is not. Therefore, our search, performed at the request of the referee, should not be interpreted as indication that we believe that the observed differences of the mean m^* is genuine.

References

Andreon, S. 2001, ApJ, 547, 623
Andreon, S. 2002, A&A, 382, 495
Andreon, S. 2006, MNRAS, 369, 969
Andreon, S. 2010, MNRAS, 407, 263 (A10)
Andreon, S. 2011a, in Astrostatistical Challenges for the New Astronomy, ed. J. Hilbe (Springer Series on Astrostatistics)
Andreon, S. 2011b, A&A, 529, L5
Andreon, S., & Ettori, S. 1999, ApJ, 516, 647
Andreon, S., & Huertas-Company, M. 2011, A&A, 526, A11
Andreon, S., Willis, J., Quintana, H., et al. 2004, MNRAS, 353, 353
Andreon, S., Punzi, G., & Grado, A. 2005, MNRAS, 360, 727
Andreon, S., Cuillandre, J.-C., Puddu, E., & Mellier, Y. 2006, MNRAS, 372, 60
Andreon, S., Puddu, E., de Propris, R., & Cuillandre, J.-C. 2008, MNRAS, 385, 979
Andreon, S., Maughan, B., Trinchieri, G., & Kurk, J. 2009, A&A, 507, 147
Andreon, S., Trinchieri, G., & Pizzolato, F. 2011, MNRAS, 412, 2391
Ashby, M. L. N., Stern, D., Brodwin, M., et al. 2009, ApJ, 701, 428
Barmby, P., Huang, J.-S., Ashby, M. L. N., et al. 2008, ApJS, 177, 431
Bertin, E., & Arnouts, S. 1996, A&AS, 117, 393
Bielby, R., Hudelot, P., McCracken, H. J., et al. 2012, A&A, 545, A23
Brodwin, M., Stern, D., Vikhlinin, A., et al. 2011, ApJ, 732, 33
Brodwin, M., Gonzalez, A. H., Stanford, S. A., et al. 2012, ApJ, 753, 162
Bruzual, G., & Charlot, S. 2003, MNRAS, 344, 1000
Chabrier, G. 2003, PASP, 115, 763
Culverhouse, T. L., Bonamente, M., Bulbul, E., et al. 2010, ApJ, 723, L78
De Propris, R., Stanford, S. A., Eisenhardt, P. R., Dickinson, M., & Elston, R. 1999, AJ, 118, 719
De Propris, R., Stanford, S. A., Eisenhardt, P. R., Holden, B. P., & Rosati, P. 2007, AJ, 133, 2209
Fassbender, R., Böhringer, H., Nastasi, A., et al. 2011, New J. Phys., 13, 125014
Gal, R. R., Lemaux, B. C., Lubin, L. M., Kocevski, D., & Squires, G. K. 2008, ApJ, 684, 933
Gobat, R., Daddi, E., Onodera, M., et al. 2011, A&A, 526, A133
Henry, J. P. 2000, ApJ, 534, 565

Henry, J. P., Salvato, M., Finoguenov, A., et al. 2010, ApJ, 725, 615
Hilton, M., Stanford, S. A., Stott, J. P., et al. 2009, ApJ, 697, 436
Hilton, M., Lloyd-Davies, E., Stanford, S. A., et al. 2010, ApJ, 718, 133
Jannuzi, B. T., & Dey, A. 1999, Photometric Redshifts and the Detection of High Redshift Galaxies, ASP Conf. Ser., 191, eds. R. Weymann, L. Storrie-Lombardi, M. Sawicki, & R. Brunner, 111
Johnston, R. 2011, A&ARv, 19, 41
Mancone, C. L., Gonzalez, A. H., Brodwin, M., et al. 2010, ApJ, 720, 284
Mancone, C. L., Baker, T., Gonzalez, A. H., et al. 2012, ApJ, 761, 141
Maraston, C. 2005, MNRAS, 362, 799
Mauduit, J.-C., Lacy, M., Farrah, D., et al. 2012, PASP, 124, 714
Meyers, J., Aldering, G., Barbary, K., et al. 2012, ApJ, 750, 1
Mullis, C. R., Rosati, P., Lamer, G., et al. 2005, ApJ, 623, L85
Muzzin, A., Wilson, G., Lacy, M., Yee, H. K. C., & Stanford, S. A. 2008, ApJ, 686, 966
Oemler, A., Jr. 1974, ApJ, 194, 1
Panuzzo, P., Silva, L., Granato, G. L., Bressan, A., & Vega, O. 2005, in The Spectral Energy Distribution of Gas-Rich Galaxies: Confronting Models with Data, eds. C. C. Popescu, & R. J. Tuffs, AIP Conf. Ser., in press [arXiv:astro-ph/0501464]
Papovich, C., Momcheva, I., Willmer, C. N. A., et al. 2010, ApJ, 716, 1503
Papovich, C., Bassett, R., Lotz, J. M., et al. 2012, ApJ, 750, 93
Pierre, M., Clerc, N., Maughan, B., et al. 2012, A&A, 540, A4
Raichoor, A., & Andreon, S. 2012a, A&A, 543, A19
Raichoor, A., & Andreon, S. 2012b, A&A, 537, A88
Sandage, A., Tammann, G. A., & Yahil, A. 1979, ApJ, 232, 352
Schechter, P. 1976, ApJ, 203, 297
Silva, L., Granato, G. L., Bressan, A., & Danese, L. 1998, ApJ, 509, 103
Snyder, G. F., Brodwin, M., Mancone, C. M., et al. 2012, ApJ, 756, 114
Stalder, B., Ruel, J., Suhada, R., et al. 2013, ApJ, 763, 93
Stanford, S. A., Eisenhardt, P. R., Brodwin, M., et al. 2005, ApJ, 634, L129
Stanford, S. A., Romer, A. K., Sabirli, K., et al. 2006, ApJ, 646, L13
Stanford, S. A., Brodwin, M., Gonzalez, A. H., et al. 2012, ApJ, 753, 164
Strazzullo, V., Rosati, P., Pannella, M., et al. 2010, A&A, 524, A17
Tanaka, M., Finoguenov, A., Mirkazemi, M., et al. 2013, PASJ, 65, 17
Tozzi, P., Santos, J. S., Nonino, M., et al. 2013, A&A, 551, A45
Zibetti, S., Gallazzi, A., Charlot, S., Pierini, D., & Pasquali, A. 2013, MNRAS, 428, 1479
Zwicky, F. 1957, Morphological astronomy (Berlin: Springer)